



BEHAVIOR OF PRESTRESSED HOLLOW CORE SLABS WITH OPENINGS STRENGTHENED WITH NEAR SURFACE MOUNTED FRP STRIPS

Omar Hesham, Mahmoud Elkateb, Ayman Khalil

Structural Engineering Department, Ain Shams University, Cairo, Egypt

ملخص البحث.

لقد اصبح التدعيم باستخدام البوليمرات المسلحة بالالياف المدفونة بالقرب من السطح من الطرق واسعة الانتشار نتيجة لوجود خصائص تماسك افضل مقارنة بباقي طرق التدعيم. قد تتعرض البلاطات سابقة الاجهاد ذات القوالب المفرغة الي تغيرات اثناء فترة التشغيل قد تستدعي وجود فتحات. قد يؤدي هذا التغيير الي التأثير علي السلوك الكلي لهذه البلاطات و بهذا تستدعي تدعيمها. تم عمل نموذج باستخدام طريقة العناصر المحددة وتم التأكد من صحتها مقارنة بالنتائج المعملية الموجودة في الابحاث السابقة. تم الحصول علي نتائج دقيقة الي حد كبير مما يجعل النموذج المقترح اساسا يمكن الاعتماد عليه للقيام بدراسات بارامترية في المستقبل لتحقيق دراسة اكثر عمقا لهذا النوع من البلاطات.

Abstract.

Strengthening with near-surface-mounted (NSM) fiber-reinforced-polymer (FRP) has become a well-known strengthening technique due to the better bond characteristics experienced compared to other strengthening techniques. The prestressed hollow core slabs (PHCS) may be subjected during their service life to changes that require the allocation of an opening. Such change may affect the overall behaviour of such slabs and thus require strengthening. A finite element model was constructed and validated against the experimental results available in the literature. A reasonably accurate result was achieved which makes the developed model a base for future parametric studies to further investigate such slabs.

1. Introduction

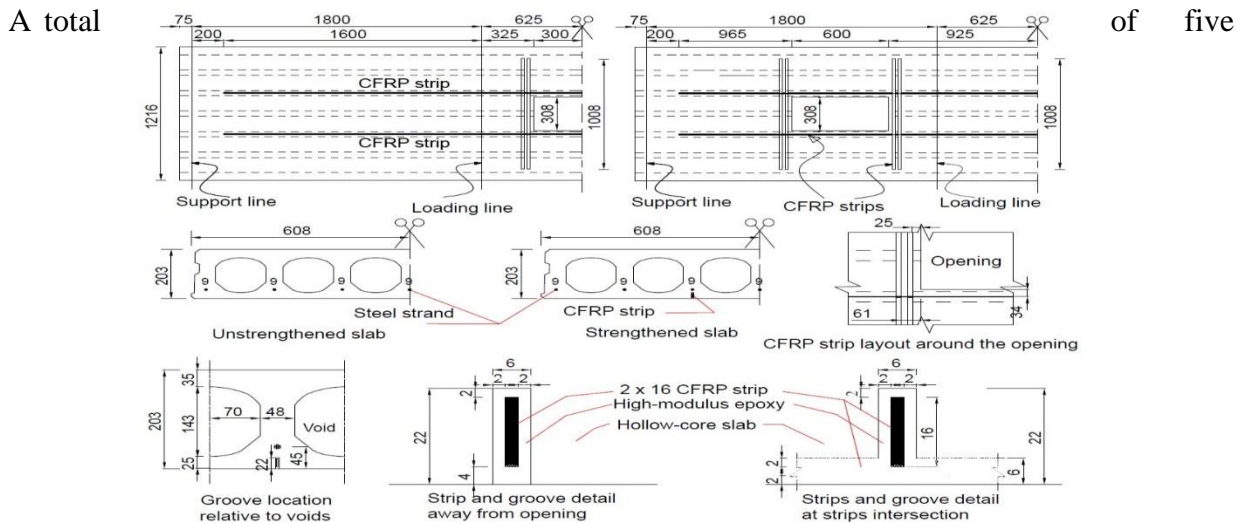
The PHCSs are produced by the extrusion process using a zero slump concrete mix. It is not practical to provide additional reinforcement rather than the prestressing strands. Thus the presence of an opening that causes the cutting of the strands may cause a noticeable reduction in the strength of the PHCSs that has to be compensated. A disturbed region occurs where a non-linear distribution of stresses takes place. In this paper, the NSM FRP strengthening technique is suggested to restore or enhance the capacity of such slabs. The NSM technique compared to the

externally bonded technique has a better protection from environmental circumstances and less susceptibility to debonding.

Elgabbas et al. [1] studied the flexural strengthening of the PHCSs in the positive moment region experimentally and analytically. NSM technique specimens experienced capacity enhancement up to 80 % while it was only 15% for EB specimens without anchorage system and 70% with mechanical anchorage system. The pre-cracking response and cracking loads of all strengthened slabs were nearly unaffected by the CFRP strengthening. The NSM strengthening technique achieved total prevention of the CFRP de-bonding brittle failure mode in opposite to the EB technique.

Pachalla et al.[2] conducted an evaluation for the effect of openings on the PHCSs. The presence of an opening significantly reduced the ultimate strength of slabs up to 44%. Opening in the slabs changed the mode of failure. Flexural opening in the shear dominated loading converted the brittle shear failure to a ductile flexural failure. Moreover, the presence of shear opening in the flexure dominated loading converted the ductile flexural failure into a more brittle shear-dominated one. Presence of opening causes stress concentration, leading to the localization of the cracks around the opening location with no distribution to the surrounding regions. Flexural opening reduced the stiffness by approximately 40%. This reduction in stiffness indicates that necessary serviceability criterion has to be checked properly when flexural openings are provided.

2. Experimental program overview



prestressed hollow-core slabs were tested to failure by Karam et al. [3]. The slabs were 5000 mm long and 203 mm thick with a concrete cross-sectional area of 140,194 mm². The slabs originally had an internal prestressing steel reinforcement ratio of 0.00274. The prestressing reinforcement consisted of seven size 9 (0.375 in.) strands. In two of the slabs, an opening was cut within the flexural span to reduce the compression area and interrupt a pretensioned strand, which was expected to reduce the flexural capacity by a not-yet-determined amount. In addition, in two other slabs, an opening was cut in the shear span to reduce the web width and to interrupt the middle

strand, which could adversely affect the shear capacity of the slab and possibly change the mode of failure. The fifth slab had no opening to serve as a reference. For each opening location, one slab was strengthened with the near-surface-mounted technique. Table 1 summarizes the specimens details and the concrete compressive strength. The CFRP strips had a modulus of elasticity of 131 GPa and a tensile strength of 2068 MPa. The epoxy adhesive had a modulus of elasticity of 3792 MPa and a tensile strength of 62 MPa.

Fig. 1. Geometry of the tested slabs and groove details at the openings

Details of specimens tested.

Specimen	Concrete Strength, MPa	Location of opening	Strengthening
NO-O	64	No opening	N/A
FO-O	64	Flexural opening	N/A
FO-S	56.5	Flexural opening	Strengthened with NSM strips
SO-O	56.5	Shear opening	N/A
SO-S	56.5	Shear opening	Strengthened with NSM strips

3. Finite element analysis

3.1. Finite element model

Finite element models were generated for the experimentally tested PHCSs. The FEM is described in details in the next sections. Two loading steps were performed. In the first one, the prestressing force is transferred to the concrete. While in the other step, the load is transferred to the loading plates and then to the PHCS.

3.2. Modelling of materials

3.2.1. Concrete constitutive model

The concrete damage plasticity model is the model used to model the concrete behavior in this study. The CDP model utilizes the models suggested by Lubliner et al. (1989) [4] and Lee and Fenves (1998) [5]. The model used by Lubliner et al. was for monotonic loading then it was developed by Lee and Fenves (1998) afterwards to consider the cyclic and dynamic loadings. The failure surface in the deviatoric cross section is not circular in shape and is governed by the Kc value as shown in **Fig. 2**. The parameters input to describe the CDP model are shown in table 2.

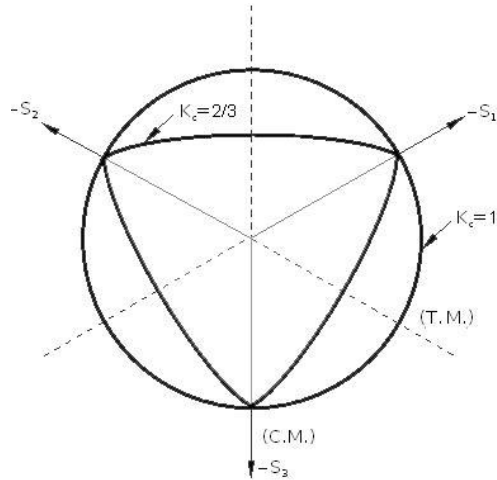


Fig. 2. Deviatoric cross section of failure surface in CDP model

The inelastic strains have to be input in the FEM programs. The next equations describe the calculations.

$$\begin{aligned} \epsilon_{cin} &= \epsilon_c - \epsilon_{cel} \\ \epsilon_c^{el} &= \frac{\sigma_c}{E_0} \end{aligned}$$

The CDP model calculates parameters for concrete damage in both compression and tension from the stress-strain values.

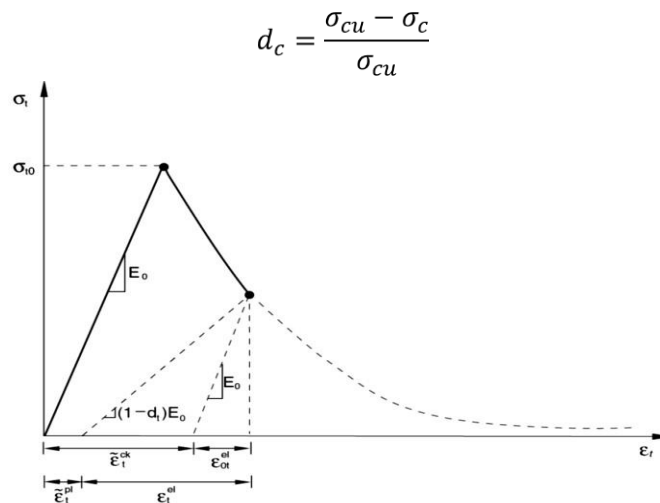


Fig. 3. Illustration of the definition of the Plastic/cracking strains used for defining the tension stiffening data (HKS 2010)

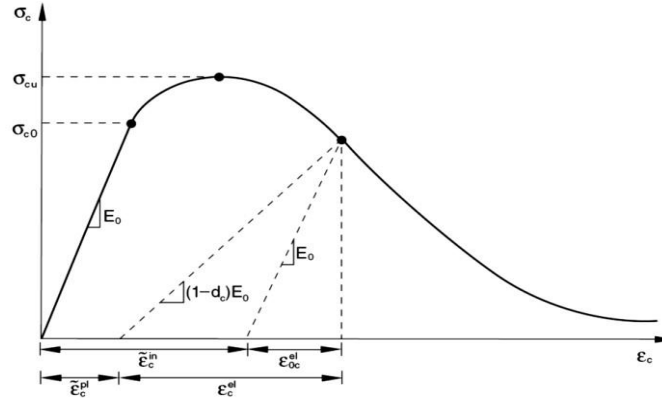


Fig. 4. Illustration of the definition of concrete crushing strains used for defining the compression data (Hibbitt et al. ,2000)

Table 2.

Parameters of CDP model.

Parameter	Value
Dilation angle (φ)	30°
Eccentricity (m)	0.1
Ratio of initial equi-biaxial compressive yield stress to initial uniaxial compressive yield stress (f_{bo}/f_c)	1.16
Ratio of the second stress invariant on the tensile meridian to the compressive meridian ($\rho_t / \rho_c = K_c$)	0.667
Viscosity parameter	0.0001

3.2.1.1 Stress strain curve for uniaxial compression

The equation of the Eurocode 2 for the stress strain curve of concrete was used in this study. The schematic representation of the relation is shown in Figure 5.

$$\frac{\sigma_c}{f_{cm}} = \frac{k\eta - \eta^2}{1 + (K-2)\eta} \quad (1)$$

Where σ_c is the concrete compressive stress, f_{cm} is the mean value of concrete cylinder compressive strength. $\eta = \varepsilon_c / \varepsilon_{c1}$, where ε_c is the concrete compressive strain and ε_{c1} is the concrete compressive stress at the maximum stress and $\varepsilon_{c1} = 0.7f_{cm}^{0.31}$. On the other hand, the value of k is given by the following relation; $k =$

$1.05E_{cm}|\varepsilon_{c1}|/f_{cm}$. **Fig. 6** shows the uniaxial stress-strain curve in compression that has been input in the FEM tool.

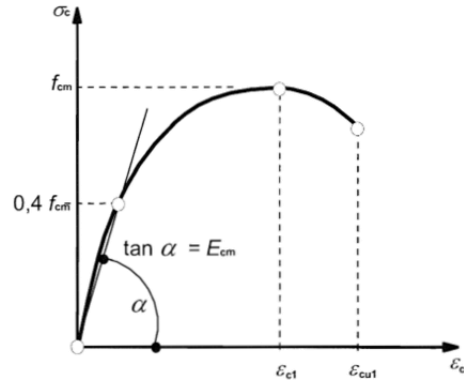


Fig. 5. Schematic representation of the relation defining the uniaxial compressive stress-strain curve (Eurocode 2 (2004))

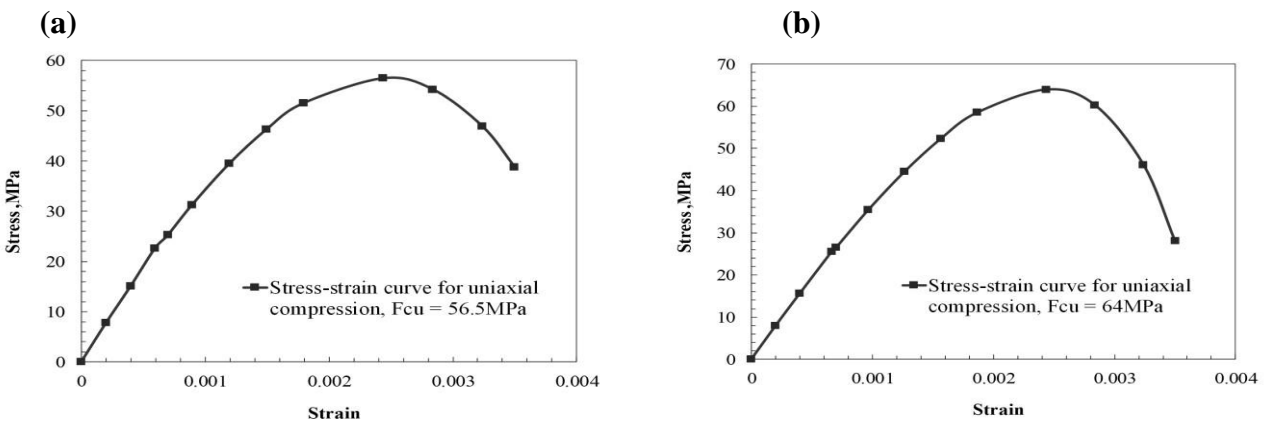


Fig. 6. (a) Stress-strain curve for uniaxial compression for specimen FO-S and (b) stress-strain curve for uniaxial compression for specimens NO-O and FO-O

3.2.1.2 Stress strain curve for uniaxial tension

The concrete tensile strength was predicted using the Eurocode 2. Before cracking, the behavior is assumed as linear elastic. Afterwards, the tension stiffening effect has to be described. Eurocode 2 (2004) evaluates the tensile strength of concrete according to Eq.2 and Eq.3.

$$f_{ctm} = 0.3 f_{ck}^{2/3} \quad (2)$$

$$f_{ctm} = 2.12 \ln(1 + (f_{cm}/10)) \quad (3)$$

Eq.5 proposed by Tamai et al. [6] to describe the tension stiffening effect was used in this study.

$$\sigma_t = E_c \varepsilon_t \text{ for } \varepsilon_t \leq \varepsilon_{cr} \quad (4)$$

$$\sigma_t = f_{ctm} \left(\frac{\varepsilon_{cr}}{\varepsilon_t} \right)^{0.4} \text{ for } \varepsilon_t > \varepsilon_{cr} \quad (5)$$

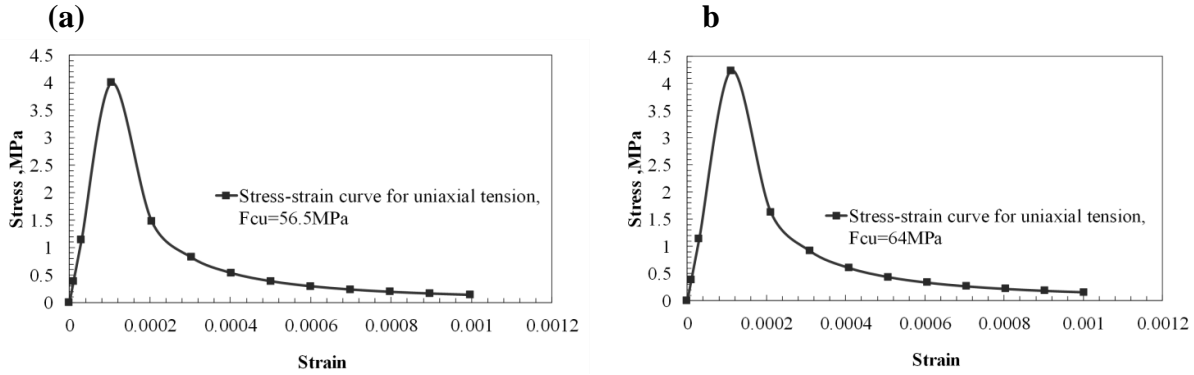


Fig. 7. (a) Stress strain curve for uniaxial tension for specimen FO-S (b) stress-strain curve for uniaxial tension

for specimens NO-O and FO-O

3.2.2. Prestressing steel reinforcement

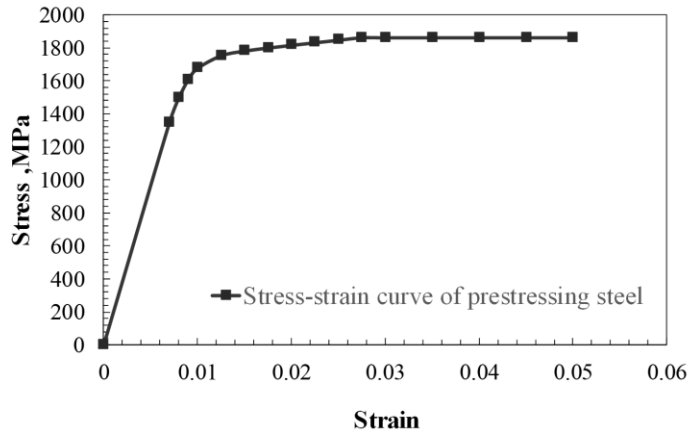
The stress-strain model developed by Devalapura and Tadros [7] for seven-wire prestressing strands. **Fig. 6** shows the stress-strain response of the prestressing strands obtained using **Eq. (7)**.

$$f_{ps} = \varepsilon_{ps} A + \frac{B}{\{1+(C\varepsilon_{ps})^D\}^{\frac{1}{D}}} \leq f_{pu} \quad (7)$$

Where f_{ps} is the stress corresponding to a given strain ε_{ps} , A, B, C & D are constants determined from **Table 3**.

Table 3.

Specimen	f_{py}/f_{pu}	A	B	C	D
1860 MPa strand	0.90	887	27613	112.4	7.360



3.2.3. CFRP strips and the epoxy adhesive

The tensile behaviour of the CFRP strip was assumed to be linear up to its ultimate tensile strength of 2068 MPa, as shown in **Fig. 9 (a)**. **Fig. 9 (b)** shows the bi-linear elastic stress-strain curve assigned to the epoxy adhesive.

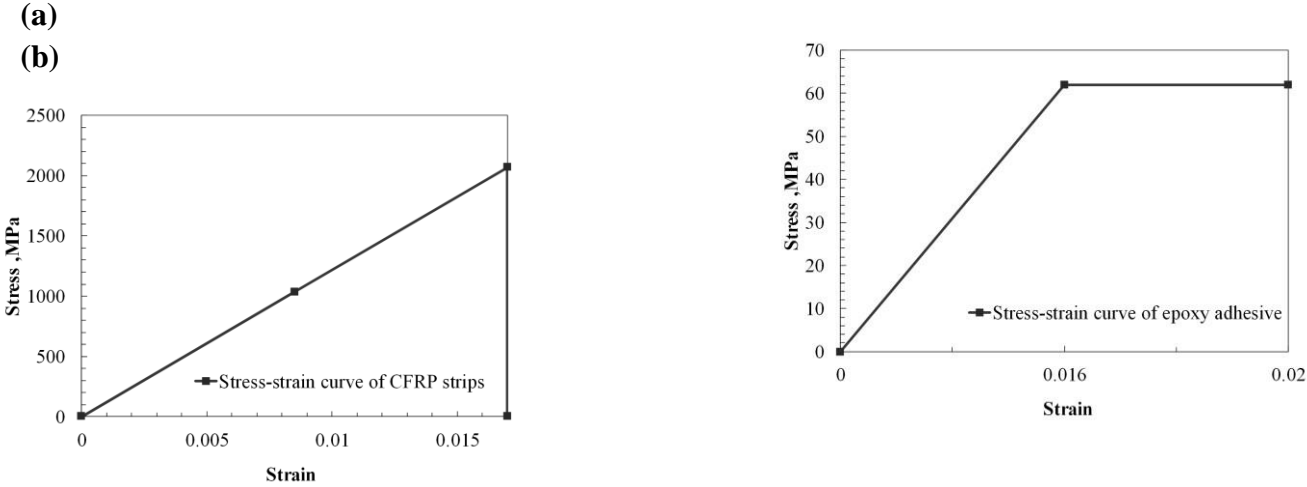


Fig. 9. Stress-strain curves: (a) CFRP strips and (b) epoxy adhesive

3.3. Element types, interactions, loading and boundary conditions

3.3.1. Element types

The concrete, epoxy adhesive, loading and supporting plates were simulated using an element type called C3D8R. The prestressing strands, CFRP strips were modelled using an element type called T3D2.

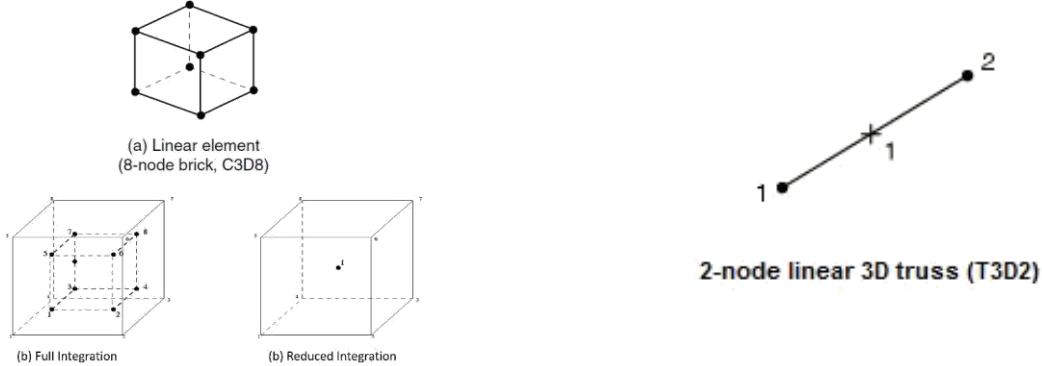


Fig. 10. Elements C3D8 and T3D2

3.3.2. Interactions

A perfect bond between the prestressing strands and the concrete was assumed. A tie constraint was used to define the interaction between the loading and support plates and the concrete.

3.4. Bond between NSM CFRP strips and concrete substrate

The relationship between the NSM CFRP strips and the concrete was assumed to be fully bonded due to the fact that the specimens experimentally tested did not experience debonding as a failure mode. However, further studies have to take the bond behavior into consideration.

4. Finite element results

4.1. Load deflection curve

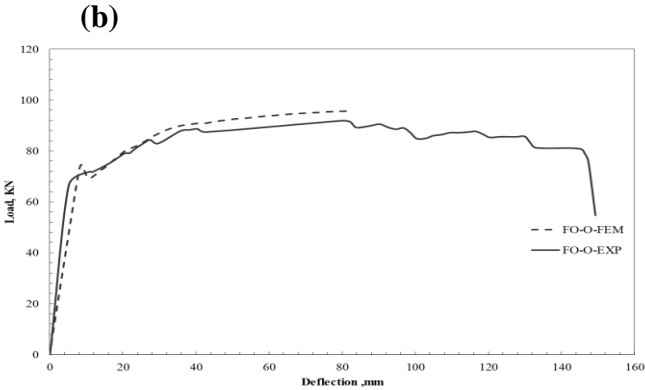
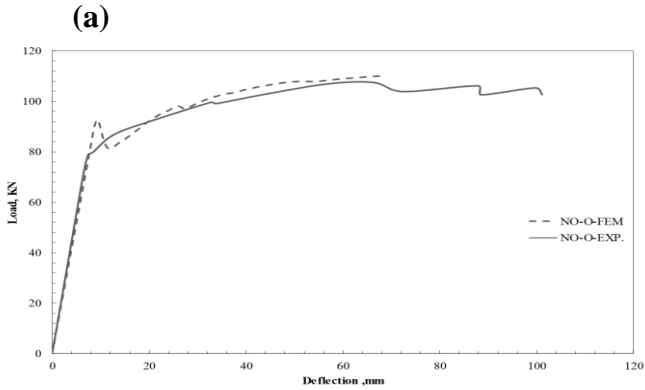
Table 4. represents a comparison between the experimental results versus the FEMs results at failure. **Fig. 9** shows the load versus deflection response experimental obtained and that predicted from the FEMs for all specimens. The developed FEMs results match the test results in terms of the load deflection response and the mode of failure.

Table 4.

Comparison of test results with the FEMs results

Specimen	Results	P_u (kN)
NO-O	FE	110
	Exp.	108
	Variation (%)	+1.85
FO-O	FE	95.7
	Exp.	92
	Variation (%)	+4.02
FO-S	FE	130.79
	Exp.	129
	Variation (%)	+1.39

Where P_u is the load at failure.



(c)

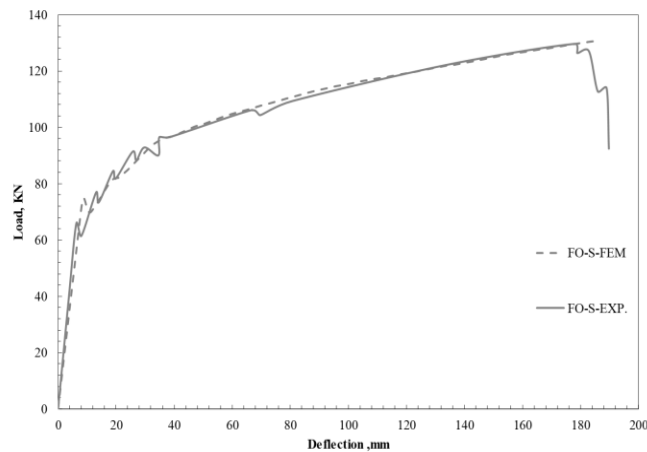


Fig. 10. Comparison between experimental and FEM results in terms of load deflection response

5. Conclusions

In this study, finite element models were constructed to predict the behavior of the PHCSs studies accurately. The FEMs were calibrated with experimental data an acceptable accuracy was achieved. The FEMs developed in this study could accurately predict the behavior of PHCSs. The maximum variation in the ultimate strength was about 4.0% compared to the experimental results. Thus, further studies to evaluate the effect of different parameters on the capacity of the PHCSs can be done using the developed calibrated model.

References

- [1] F. Elgabbas, A. A. El-Ghandour, A. A. Abdelrahman, and A. S. El-Dieb, “Different CFRP strengthening techniques for prestressed hollow core concrete slabs: Experimental study and analytical investigation,” *Compos. Struct.*, vol. 92, no. 2, pp. 401–411, 2010.
- [2] S. K. S. Pachalla and S. S. Prakash, “Experimental evaluation on effect of openings on behavior of prestressed precast hollow-core slabs,” *ACI Mater. J.*, vol. 114, no. 2, pp. 427–436, 2017.
- [3] K. Mahmoud, S. Foubert, and E. El-Salakawy, “Strengthening of prestressed concrete hollow-core slab openings using near-surface-mounted carbonfiber-reinforced polymer reinforcement,” *PCI J.*, vol. 62, no. 4, pp. 45–57, 2017.
- [4] “Lubliner_et_al_1989a_3657_LuOllOliOn1989.pdf.”
- [5] J. Lee and G. L. Fenves, “Plastic-damage model for cyclic loading of concrete structures,” *J. Eng. Mech.*, vol. 124, no. 8, pp. 892–900, 1998.
- [6] I. N. Post-yield and I. N. Uniaxial, “By Shinichi TAMAI , Hiroshi SHIMA , Junichi IZUMO and Hajime OKAMURA.”
- [7] R. K. Devalapura and M. K. Tadros, “Stress-Strain Modeling of 270 ksi Low-Relaxation Prestressing Strands,” *PCI J.*, vol. 37, no. 2, pp. 100–106, 1992.